



Universiteit
Leiden
The Netherlands

**Exploring and modulating the tumor immune microenvironment:
Towards improving patient outcomes of immunotherapy in lung cancer**
Theelen, W.S.M.E.

Citation

Theelen, W. S. M. E. (2020, October 21). *Exploring and modulating the tumor immune microenvironment: Towards improving patient outcomes of immunotherapy in lung cancer*. Retrieved from <https://hdl.handle.net/1887/137007>

Version: Publisher's Version

License: [Licence agreement concerning inclusion of doctoral thesis in the Institutional Repository of the University of Leiden](#)

Downloaded from: <https://hdl.handle.net/1887/137007>

Note: To cite this publication please use the final published version (if applicable).

Cover Page



Universiteit Leiden



The handle <http://hdl.handle.net/1887/137007> holds various files of this Leiden University dissertation.

Author: Theelen, W.S.M.E.

Title: Exploring and modulating the tumor immune microenvironment: Towards improving patient outcomes of immunotherapy in lung cancer

Issue date: 2020-10-21

PART I.

Exploring the tumor immune microenvironment

Willemijn S.M.E. Theelen^{1*}, Thomas Kuilman^{2*}, Katja Schulze³, Wei Zou⁴, Oscar Krijgsman², Dennis D.G.C. Peters⁵, Sten Cornelissen⁵, Kim Monkhorst⁶, Pranamee Sarma³, Teiko Sumiyoshi³, Lukas C. Amler³, Stefan M. Willems⁷, Johannes L.G. Blaauwgeers⁸, Carel J.M. van Noesel⁹, Daniel S. Peeper^{2#}, Michel M. van den Heuvel^{10#}, Marcin Kowanetz^{3#}

¹ Department of Thoracic Oncology, The Netherlands Cancer Institute, Amsterdam, The Netherlands; ² Division of Molecular Oncology & Immunology, The Netherlands Cancer Institute, Amsterdam, The Netherlands; ³ Oncology Biomarker Development, Genentech Inc., South San Francisco, USA; ⁴ Biostatistics, Genentech Inc., South San Francisco, USA; ⁵ Core Facility Molecular Pathology & Biobanking, Department of Molecular Pathology, The Netherlands Cancer Institute, Amsterdam, The Netherlands; ⁶ Division of Pathology, The Netherlands Cancer Institute, Amsterdam, the Netherlands; ⁷ Department of Pathology, University Medical Centre Utrecht, Utrecht, The Netherlands; ⁸ Department of Pathology, OLVG, Amsterdam, The Netherlands; ⁹ Department of Pathology, Academic Medical Center, Amsterdam, The Netherlands; ¹⁰ Department of Pulmonology, Radboud University Medical Center, Nijmegen, The Netherlands

*These authors contributed equally to this work

#These authors also contributed equally to this work

CHAPTER 2

Absence of PD-L1 expression on tumor cells in the context of an activated immune infiltrate may indicate impaired IFN γ signaling in non-small cell lung cancer

PLoS One. 2019 May 24;14(5):e0216864

ABSTRACT

Background

In non-small cell lung cancer (NSCLC), PD-L1 expression on either tumor cells (TC) or both TC and tumor-infiltrating immune cells (IC) is currently the most used biomarker in cancer immunotherapy. However, the mechanisms involved in PD-L1 regulation are not fully understood. To provide better insight in these mechanisms, a multiangular analysis approach was used to combine protein and mRNA expression with several clinicopathological characteristics.

Patients and methods

Archival tissues from 640 early stage, resected NSCLC patients were analyzed with immunohistochemistry for expression of PD-L1 and CD8 infiltration. In addition, mutational status and expression of a selection of immune genes involved in the PD-L1/PD-1 axis and T-cell response was determined.

Results

Tumors with high PD-L1 expression on TC or on IC represent two subsets of NSCLC with minimal overlap. We observed that PD-L1 expression on IC irrespective of expression on TC is a good marker for inflammation within tumors. In the tumors with the highest IC expression and absent TC expression an association with reduced IFN γ downstream signaling in tumor cells was observed.

Conclusions

These results show that PD-L1 expression on TC and IC are both independent hallmarks of the inflamed phenotype in NSCLC, and TC-negative/IC-high tumors can also be categorized as inflamed. The lack of correlation between PD-L1 TC and IC expression in this subgroup may be caused by impaired IFN γ signaling in tumor cells. These findings may bring a better understanding of the tumor-immune system interaction and the clinical relevance of PD-L1 expression on IC irrespective of PD-L1 expression on TC.

INTRODUCTION

One of the most studied tumor immune escape mechanisms is mediated through the inhibitory programmed death-ligand 1 (PD-L1)/programmed death 1 (PD-1) pathway. The development of anti-PD-L1/PD-1 monoclonal antibodies has led to long-lasting anti-tumor immune responses in a subset of patients with non-small cell lung cancer (NSCLC). High PD-L1 expression as assessed by immunohistochemistry (IHC) has consistently been reported to be associated with higher responses to anti-PD-L1/PD-1 treatment, resulting in the development of various diagnostic PD-L1 IHC assays [1–3]. The use of various diagnostic PD-L1 IHC assays has led to ambiguity as to how to use this multi-faceted biomarker. In two randomized trials comparing the anti-PD-L1 antibody atezolizumab to docetaxel in second line setting, PD-L1 expression on TC and on infiltrating immune cells (IC) both appeared to be independently associated with response to atezolizumab [3, 4].

Besides PD-L1 expression, wider aspects of the tumor/immune-infiltrating complex are under investigation as biomarkers for immunotherapy. Tumors can broadly be divided into inflamed (hot) vs non-inflamed (cold) tumors. Typically, inflamed tumors show a pre-existing antitumor immune response with abundance of tumor-infiltrating lymphocytes (TILs), IFN γ -producing CD8 $^+$ T-cells and high expression of PD-L1. In contrast, non-inflamed tumors are characterized as immune desert: containing hardly any TILs and rarely expressing PD-L1 [5, 6]. The development of gene expression profiling of tumors allows distinguishing 'hot' and 'cold' tumors by providing prognostic and predictive immune signatures; one example being the T-effector (T $_{eff}$) signature showing an association with efficacy in the randomized phase II and III trials comparing atezolizumab to docetaxel [3, 4].

Hence, it is important to improve insights in the overlap and differences between PD-L1 expression on TC and/or IC and to relate this expression to other tumor features and markers of the PD-L1/PD-1 axis and T-cell response. In order to do this, we used a multiangular approach by combining protein and mRNA expression with clinicopathological characteristics, including mutational analysis of well-known drivers of NSCLC in a large cohort of clinically annotated resected NSCLC samples.

MATERIALS AND METHODS

Sample collection and patient cohort

Inclusion criteria for this cohort were patients that had undergone a lung resection between 1990 and 2013 at one of four Dutch medical centers. Exclusion criteria were a synchronous primary tumor, unavailability of tumor tissue or patient follow-up data, histology of non-NSCLC, e.g. SCLC or metastasized non-NSCLC. Clinical data about gender, smoking status, neo-adjuvant and adjuvant treatment, age at resection, type of resection, tumor stage, progression free survival (PFS) and overall survival (OS) were collected. No data on treatment after relapse of disease was available. The cohort included 768 samples with adequate patient and tumor characteristics. For all these patients, formalin-fixed, paraffin-embedded (FFPE) tumor samples were collected. After a second pathology revision, samples without sufficient vital tumor material were excluded, leaving 640 samples eligible for further

analysis. All tumors were histopathologically classified according to the 2015 WHO classification system [7]. TNM classification was redefined for resections that were done before 2010 according to the 7th lung cancer TNM classification and staging system. Smoking status was defined by pack years (PY). Light smokers were defined by having less than 10 PY, including never smokers. Prior to analysis the samples were de-identified. The Translational Research Board of the Netherlands Cancer Institute-Antoni van Leeuwenhoek hospital approved the use of patient data and material in this study.

Immunohistochemical staining, mutational and gene expression analysis

PD-L1 expression and CD8 staining was assessed in a central laboratory (HistoGeneX, Belgium) using whole slide sections prepared from FFPE resection specimens. Sections were stained using the rabbit anti-human anti-PD-L1 antibody (clone SP142, Spring Bioscience) and the monoclonal mouse anti-human anti-CD8 antibody (clone C8/144B, DAKO) on a Ventana BenchMark XT autostainer (Ventana Medical Systems). PD-L1 expression in TC was assessed as the proportion of TC showing membrane staining of any intensity; expression in IC was assessed as the proportion of tumor area occupied by PD-L1-positive IC of any intensity (Figure 1A-B and S1) [3, 4]. In all specimens, total immune infiltrate and tumor cells were assessed in the tumor area by a certified pathologist based on hematoxylin background staining of the IHC slide and if needed based on the H&E staining. Positive and negative controls were performed using tonsil tissue. The scoring algorithm was developed for the approved VENTANA PD-L1 (SP142) Assay and further details concerning the PD-L1 staining protocol have been described previously [8, 9]. PD-L1 score for expression on TC and IC was available for 615 (96.1%) samples. CD8 staining was reported as the percent CD8-positive tumor infiltrating immune cells in the tumor center, available for 615 (96.1%) samples.

Mutation analysis was performed using a microfluidics-based PCR platform running an allele-specific multiplex test as previously described [10, 11]. The validated panel included a total of 130 hot spot mutations (Table S1). Immunohistochemistry for ALK was performed on a BenchMark Ultra autostainer (Ventana Medical Systems) using clone 5A4 (Abcam). For ALK FISH staining and analysis of the results was performed as described by the manufacturer.

DNA was extracted using the Qiagen DNA mini kit (cat. No. 51306) and a minimum of 80ng DNA was shipped to Genentech Inc. for mutation analysis. Gene expression analysis was performed using the NanoString nCounter Analysis system (NanoString) on 80-200ng RNA extracted from FFPE tissue samples. A customized gene panel, including 795 targets including multiple genes of immunologic function and cancer biology and including 4 housekeeping genes was applied. Following thorough assay quality control, data were normalized and underwent analysis. We report here results for CD8 (*CD8A*), PD-L1 (*CD274*), PD-1 (*PDCD1*), PD-L2 (*PDCD1LG2*) and T_{eff} signature that was defined as the mean expression for *CD8A*, *GZMA*, *GZMB*, *IFNG*, *EOMES*, *CXCL9*, *CXCL10* and *TBX21* as previously described [3, 4]. The downstream IFN γ response signature was derived from the DER_IFN_GAMMA_RESPONSE_UP gene set (MSigDB; <http://software.broadinstitute.org/gsea/msigdb>; 71 genes), where signature expression was calculated by summing the log₂-based expression values for genes that are members of the gene set and that are present in the expression data (22 / 71 genes). To calculate the actual minus the expected (residual)

IFN γ signature expression, a linear model based on all samples was created describing the relationship between downstream IFN γ response signature and T_{eff} signature expression. This model was used to calculate the expected IFN γ signature expression. Biomarker high and low subgroups were defined by expression levels at or above various cut-offs, either above or below the median or above or below the 25% or 75% quantile. Gene expression analysis was available for 530 (82.8%) of the samples.

Statistical analysis

All statistical tests were performed in R. Kaplan–Meier methodology was used to construct survival curves. Stratified Cox regression models were used to estimate HRs and 95% CIs in biomarker subgroup populations. For comparison of gene expression data among subgroups, (pairwise) t-tests were performed. For comparison of protein expression data among subgroups, (pairwise) Wilcoxon rank sum tests were performed. For comparison of categorical data among subgroups, Fisher's exact tests or Pearson's Chi-squared tests were used as indicated. The false discovery rate (FDR) was controlled below 0.05 using Benjamini-Hochberg method.

RESULTS

Description of the cohort and distribution of PD-L1 protein expression and CD8 infiltration

The cohort consisted of 640 NSCLC samples: 344 (53.8%) AC, 267 (41.8%) SCC and 29 (4.5%) NSCLC NOS. Only 48 (7.5%) patients were light or never smokers. 83.9% of the cohort was early stage disease (\leq stage II). Median follow-up time was 96.0 months (95% CI: 86–103). All samples were screened for presence of an ALK translocation or mutations of well-known drivers in NSCLC. Mutational analysis was available for 563 (88.0%) samples: 170 mutations were found in 164 patients (29.1%). Six samples harbored two mutations. ALK IHC was available for 630 (98.4%) samples. Four samples (0.6%) were ALK IHC positive and a translocation was confirmed by FISH. *EGFR*, *KRAS*, *BRAF* and *ALK* aberrations were mutually exclusive. Table 1 summarizes the clinicopathological characteristics and genetic alterations of our patient cohort.

In order to investigate the overlap and differences of PD-L1 protein expression between TC and IC, all samples were scored for PD-L1 expression on TC and on IC at all four expression levels. Examples of PD-L1 staining, PD-L1 IHC scoring criteria, the overall prevalence and distribution by overlapping PD-L1 subgroups are presented in Figure 1A–1D and S1. Non-overlapping PD-L1 subgroups are presented in Figure S2. High PD-L1 expression (TC3 or IC3) was present in 132 (21.5%) samples and 74 (12.0%) samples showed no PD-L1 expression (TC0 and IC0 subgroup) (Figure 1C). Only a minority of samples (10.4%) had CD8 infiltration in the tumor center of 5% or higher (Figure 1E).

Inflammatory features like PD-L1 expression may be affected by traditional stratifying criteria (i.e. gender, age, smoking status, histology, tumor stage or *KRAS/EGFR* status). In a univariate analysis using the TC and IC scores separately a positive association between heavy smoking and PD-L1 expression on TC ($p = 0.016$) was found, but not for PD-L1 expression on IC. There was no significant difference in PD-L1 expression between the histologic subtypes (Figure S3A–D). PD-L1 expression on

TC was significantly higher for *KRAS* mutant (*KRAS_m*) tumors compared to *KRAS* wild type (*KRAS_{wt}*) tumors ($p < 0.001$) and this was irrespective of smoking status. No difference was found for PD-L1 expression on IC by *KRAS* status (Figure S3E-F). *EGFR_m* status was not significantly associated with PD-L1 protein expression (data not shown).

The correlation between PD-L1 protein expression and PD-L1 mRNA expression (encoded by *CD274*) was investigated. Protein expression of both TC and IC was significantly associated with mRNA expression of *CD274* (Figure S4).

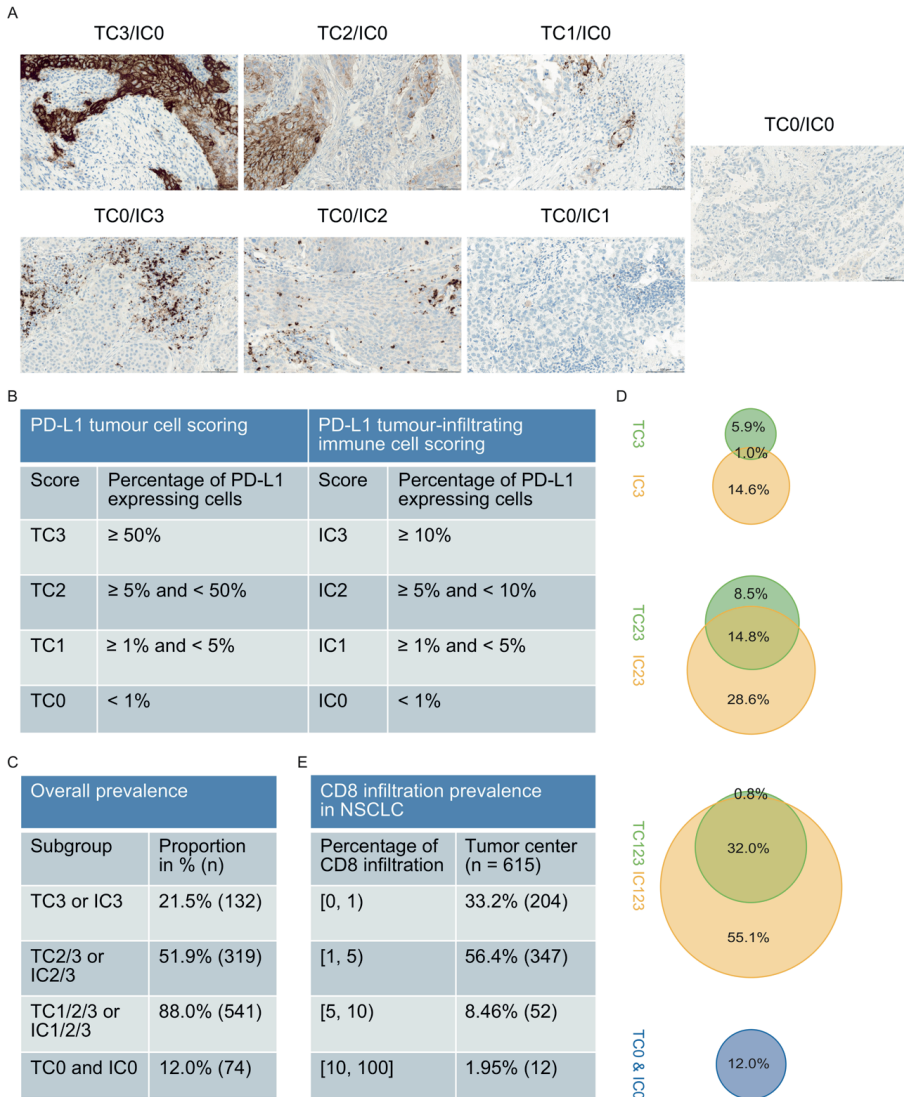
Table 1. Patients' and tumor characteristics of the non-small cell lung cancer cohort.

Total (n = 640)	AC 344	SCC 267	NSCLC NOS 29
Gender			
Male	163 (47.3%)	188 (70.4%)	17 (58.6%)
Female	181 (52.7%)	79 (29.6%)	12 (41.4%)
Median age at surgery (years, range)	62 (30-84)	67 (38-85)	57 (37-81)
Neo-adjuvant therapy	54 (15.7%)	13 (4.9%)	7 (24.1%)
Chemotherapy	21 (6.1%)	2 (0.7%)	1 (3.4%)
Concurrent chemo radiotherapy	8 (2.3%)	2 (0.7%)	4 (13.8%)
Sequential chemo radiotherapy	3 (0.9%)	0	0
Erlotinib [[56]]	22 (6.4%)	6 (2.2%)	2 (6.9%)
Radiotherapy	0	3 (1.1%)	0
No neo-adjuvant therapy	290 (84.3%)	254 (95.1%)	22 (75.9%)
Adjuvant treatment			
Chemotherapy	49 (14.2%)	45 (16.9%)	8 (27.6%)
Radiotherapy	19 (5.5%)	24 (9.0%)	2 (6.9%)
Chemotherapy + radiotherapy	7 (2.0%)	9 (3.4%)	1 (3.4%)
No adjuvant therapy	244 (70.9%)	160 (59.9%)	14 (48.3%)
Unknown	25 (7.3%)	29 (10.9%)	4 (13.8%)
Smoking			
Light smokers <10PY	42 (12.2%)	4 (1.5%)	2 (6.9%)
Heavy smokers ≥10PY	253 (73.5%)	224 (83.9%)	25 (86.2%)
Unknown	49 (14.2%)	39 (14.6%)	2 (6.9%)
Tumor stage at resection			
Stage I	211 (61.3%)	131 (49.0%)	13 (44.8%)
Stage II	79 (23.0%)	95 (35.6%)	9 (31.0%)
Stage III	44 (12.8%)	34 (12.7%)	7 (24.1%)
Stage IV	10 (2.9%)	7 (2.6%)	0
Genetic alterations*			
EGFR mutated	20 (6.3%)	1 (0.5%)	0
KRAS mutated	110 (34.6%)	7 (3.4%)	3 (10.3%)
ALK translocated	4 (1.3%)	0	0
PIK3CA mutated	10 (3.1%)	14 (6.8%)	0
BRAF mutated	1 (0.3%)	0	0
NRAS mutated	1 (0.3%)	2 (1.0%)	0
HRAS mutated	1 (0.3%)	0	0
No mutation detected	171 (53.8%)	182 (88.3%)	26 (89.7%)
Undetermined [^]	26	61	0
Mean overall survival (months, range)	71 (0-285)	76 (0-289)	71 (6-273)

* percentages for analyzed samples only. *EGFR* mutations included exon 19 deletions (n=15), exon 20 insertions (n=2) and exon 21 L858R mutations (n=4). No T790M mutations were found. *KRAS* mutations included mutations in codon 12 and 13 (n=116) and codon 61 (n=4). Mutations in *AKT1*, *ERBB2*, *FLT3*, *JAK2*, *KIT*, *MYD88* were not present within this cohort. All present *MET* mutations (n=30) were germline single nucleotide polymorphism (SNP). [^] mutation status was undetermined when no sufficient DNA was available or when the microfluidics-based PCR platform lead to an invalid result.

SCC = squamous cell carcinoma, AC = adenocarcinoma, NSCLC NOS = non-small cell lung cancer not otherwise specified, PY = pack years

Figure 1. Examples of PD-L1 staining, scoring criteria, prevalence and overlap between PD-L1 expression on TC and IC and prevalence of CD8 infiltration in the tumor center in NSCLC.



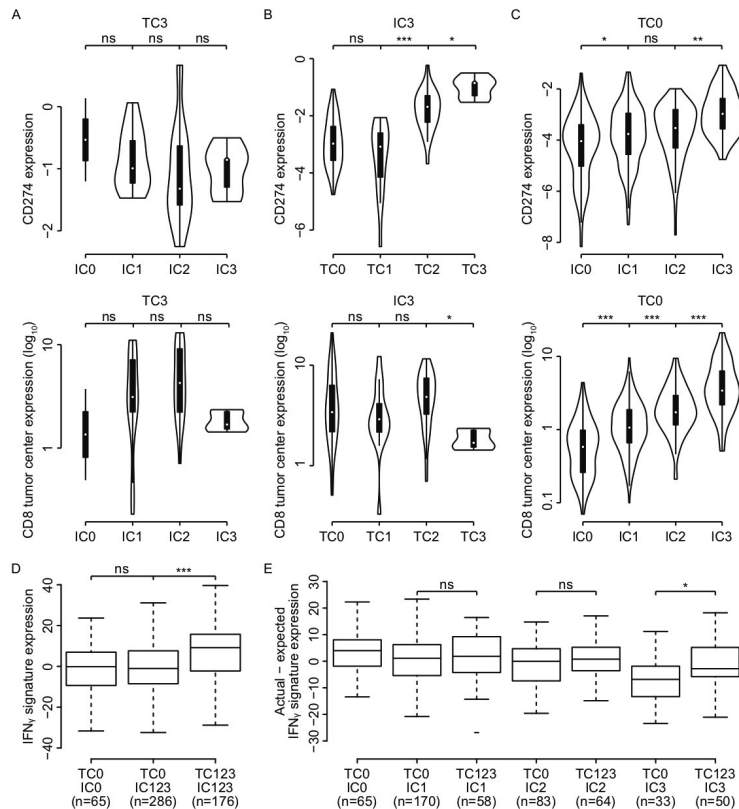
(A) PD-L1 expression by IHC on both TC and IC for each subgroup. (B) PD-L1 IHC scoring criteria on TC and IC [57] (C) Overall prevalence of overlapping PD-L1 subgroups. (D) Percentages in Venn diagrams represent the prevalence of PD-L1 expression by TC and IC in overlapping subgroups. (E) Overall prevalence of CD8 infiltration in the tumor center.

Overlap and differences of PD-L1 protein expression on TC and IC

We then explored the distribution of PD-L1 expression and the overlap and differences between expression on TC and IC. There was minimal overlap between TC3 and IC3 tumors (1.0%, Figure 1D), which might suggest different mechanism of PD-L1 upregulation in tumor cells compared to immune cells. Comparing TC3 tumors to IC3 tumors in regard to clinicopathological features did not reveal significant differences (Table S2). Next, we analyzed potential differences with respect to immunological

features. To correct for potential confounding of the true biology of TC3 and IC3 tumors by the PD-L1 expression in the other compartment, we compared TC3 tumors based on various expression levels of IC (0 to 3) to IC3 tumors based on various expression levels of TC (0 to 3) (Figure 2A–2C and S5). In the TC3 subgroup ($n = 39$), expression of all inflammatory markers showed a slight increase per increasing IC subgroup except expression of *CD274*, but this was not significant. In the IC3 subgroup ($n = 83$), we found that only expression of *CD274* increased per increasing TC score, while the other inflammatory markers remained constant, i.e. CD8 infiltration, T_{eff} signature, *CD8A*, *PDCD1* and *PDCD1LG2* expression. Also, when evaluating TC0 samples based on various levels of IC (0 to 3; $n = 351$) all inflammatory markers, including *CD274*, increased per ascending IC subgroup. The IC score therefore seems to represent a characteristic of true ‘hot’ tumors.

Figure 2. Associations of mRNA expression of *CD274*, infiltration of CD8 and the IFN γ response signature in non-overlapping PD-L1 expressing subgroups.



(A) Relative mRNA expression of *CD274* and CD8 infiltration in TC3 tumors based on various levels of IC ($n = 39$). (B) Relative mRNA expression of *CD274* and CD8 infiltration in IC3 tumors based on various levels of TC ($n = 83$). (C) Relative mRNA expression of *CD274* and CD8 infiltration in TC0 tumors based on various levels of IC ($n = 351$). (D) Relative mRNA expression of the IFN γ response signature in non-overlapping PD-L1 subgroups: TC0/IC0, TC0/IC123 and TC123/IC123 ($n = 530$). (E) The actual minus the expected relative mRNA expression of the IFN γ response signature comparing TC negative to TC positive samples for each non-overlapping IC-subgroup. Expected IFN γ response signature expression was obtained from the level of T_{eff} signature expression based on their linear relationship. ns = non significant, * $p = 0.01 - 0.05$, ** $p < 0.01$, *** $p < 0.001$

As the TC0/IC123 subgroup (n = 286, 55.1%) contains the majority of samples in this cohort (Figure 1D), we then sought to understand why tumors harboring an active immune infiltrate showed no upregulation of PD-L1 on TC. Since IFN γ signaling is an important mechanism for PD-L1 upregulation, we hypothesized that an impairment in downstream IFN γ signaling within tumor cells might explain this phenomenon. It is expected that cytokine production by an active immune infiltrate, represented by the T_{eff} signature, will lead to downstream IFN γ signaling within tumor cells. Therefore, we determined the expression of selected IFN γ target genes, and collectively represented them as an IFN γ response signature. The expression of this IFN γ response signature was significantly lower in TC negative samples compared to TC positive samples (p < 0.001, Figure 2D). As this difference was irrespective of the expression of the IFN γ target PD-L1 on IC, this strongly suggests that expression of this IFN γ response signature originated from tumor cells only and not the immune infiltrate. The T_{eff} and the IFN γ response signature showed a linear relationship (Figure S6). We calculated the difference between the expected level of the IFN γ response signature based on this linear model and the actual one (residuals). To overcome confounding by the IC score, again we compared the residuals in TC0 tumors based on various subgroups of IC (0 to 3) (Figure 2E). In the TC0/IC3 subgroup, we observed a significantly lower expression of IFN γ response as would be expected by the linear model compared to the TC123/IC3 subgroup (p = 0.042). Expected expression in the TC0/IC3 subgroup was lower compared to all other subgroups. This suggests that the absence of PD-L1 expression on tumor cells in TC0/IC3 samples may be caused by impaired IFN γ signaling in these tumor cells.

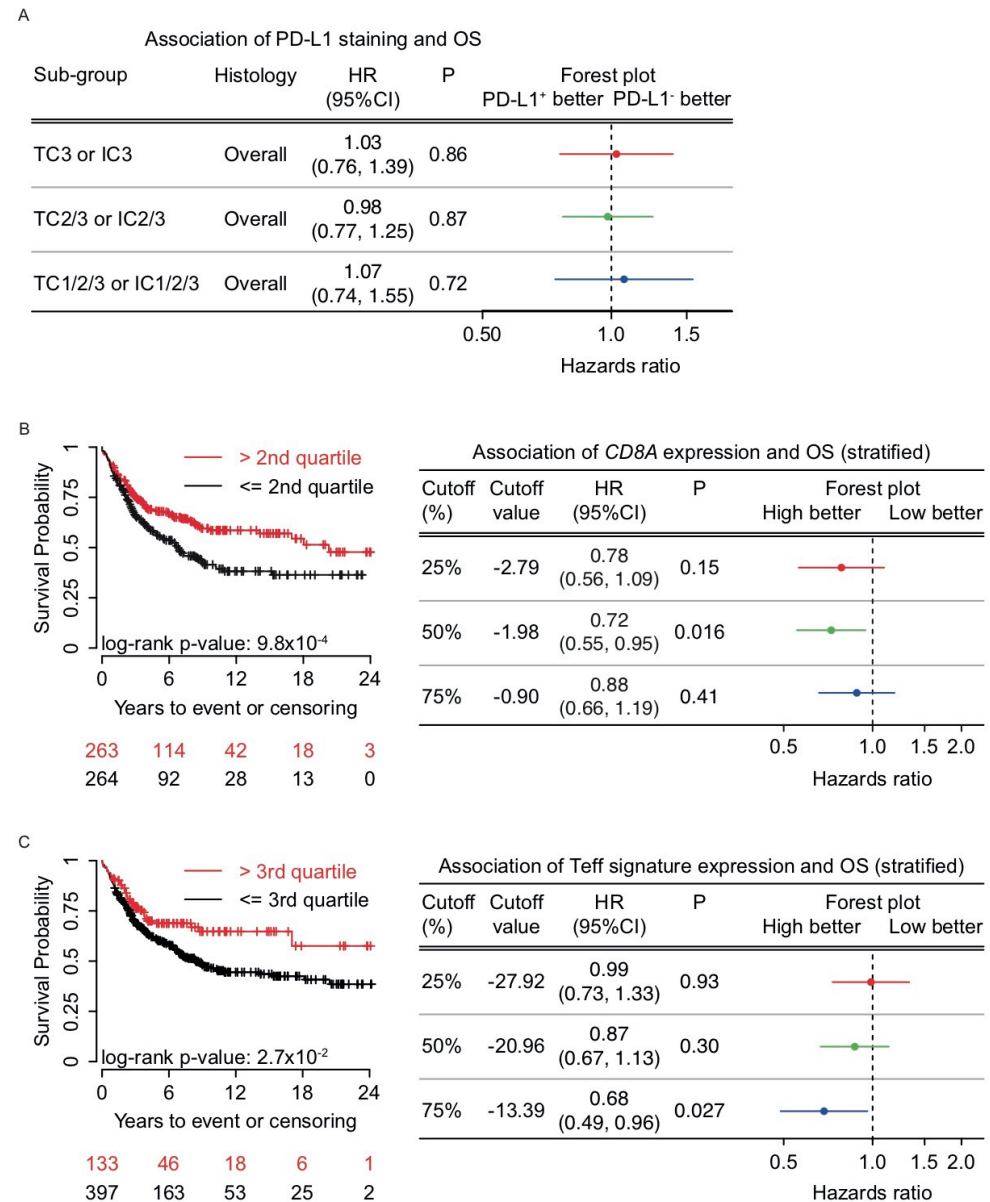
Prognostic value of PD-L1 expression, CD8 infiltration and gene expression

Recent data showed conflicting results concerning the prognostic value of PD-L1 expression in NSCLC. After stratifying for tumor stage, we analyzed the prognostic value of several inflammatory parameters measured in our cohort. PD-L1 protein expression -combined or on TC/IC separately- and mRNA expression of *CD274* had no effect on OS in our cohort (Figure 3A). CD8 infiltration by IHC only showed a trend towards improved OS, but *CD8A* transcript levels were significantly associated with better OS (HR 0.72 (95%CI 0.55–0.95; p = 0.016, Figure 3B). High expression of the T_{eff} signature (highest quartile) and *PDCD1* (highest quartile) were both positive prognostic markers (HR 0.68 (95%CI 0.49–0.96; p = 0.027), Figure 3C and HR 0.60 (95%CI 0.42–0.85; p = 0.0035), data not shown, respectively). Expression of *PDCD1LG2* or the IFN γ response signature had no OS relevance. Based on these results, we conclude that gene expression profiling is a better indicator of prognosis than PD-L1 protein expression.

DISCUSSION

To date, PD-L1 protein expression on tumor cells and on tumor infiltrating immune cells is the most studied biomarker in cancer immunotherapy. This study sought to improve insights in the relation of PD-L1 protein expression with traditional stratifying criteria, like histology and oncogenic driver status, and other markers of the PD-L1/PD-1 axis and T-cell response.

Figure 3. The effect of PD-L1 expression, the expression of *CD8A* and the T_{eff} signature on OS.



(A) Forest plot for overlapping PD-L1 expressing subgroups show no improved OS for higher PD-L1 expression; stratified for tumor stage. (B) Forest plot and Kaplan Meier curve for *CD8A* expression show improved OS for the highest two quartiles; stratified for tumor stage (HR 0.72 (95%CI 0.55-0.95; $p = 0.016$)). (C) Forest plot and Kaplan Meier curve for quartiles of the T_{eff} signature show improved OS for the highest quartile; stratified for tumor stage (HR 0.68 (95%CI 0.49-0.96; $p = 0.027$)).

In our cohort, the pattern of inflamed tumors was clearly established: expression of PD-L1 on either TC or IC, infiltration of CD8⁺ cells and mRNA expression of *CD274*, *CD8A*, *PDCD1*, *PDCD1LG2* and the T_{eff} signature were all associated with one another. Besides this overlap in inflamed features, also differences between PD-L1 expression on TC and IC were found. Co-expression of PD-L1 at the highest level on both TC and IC rarely occurred: prevalence of TC3&IC3 population was only 1%. Fehrenbacher et al. also described this lack of overlap in advanced NSCLC and hypothesized an intrinsic mechanism of PD-L1 upregulation on TC versus an adaptive mechanism on IC [3]. Unfortunately, as opposed to the studies in advanced NSCLC, this early stage cohort contained very few TC123/IC0 samples (< 1%). Therefore, our analyses had several limitations because of the risk of confounding by the PD-L1 expression in the other compartment as we could not compare the true PD-L1 TC positive (TC123/IC0) to the true PD-L1 IC positive (TC0/IC123) tumors. By comparing IC3 tumors based on various levels of TC and TC3 as well as TC0 tumors based on various levels of IC, we observed that inflammatory markers like *CD8A* and the T_{eff} signature correlated most clearly with the IC score. Not unsurprisingly, this was strongest within the TC0 subgroup and shows that the IC score is a good measure for true 'hot' tumors.

By dividing our cohort into three non-overlapping subgroups -TC0&IC0, TC0/IC123 and TC123/IC123- we were able to explore other differences between PD-L1 expression on TC vs IC. We found a significantly lower IFN γ response signature expression in TC negative versus TC positive tumors, suggesting an inability of the tumor cells to upregulate PD-L1 in the presence of an active and IFN γ producing immune infiltrate as is represented by expression of the T_{eff} signature. And as expected after performing further analysis between TC negative and TC positive samples in increasing IC subgroups, strong evidence of a hampered IFN γ -PD-L1 axis in tumor cells within the TC0/IC3 subgroup was found. As to our knowledge, this finding has not been described or looked into before. We observed impaired expression of the majority of the individual IFN γ response signature genes (data not shown), implying that the impaired IFN γ signaling in TC0/IC3 tumors is due to alterations at an early level of the pathway: IFNGR or JAK/STAT. Kowanetz et al. found that the TC0/IC3 subgroup had a response rate to the PD-L1 inhibitor atezolizumab of 22%, which was higher than TC0&IC0 tumors (ORR 8%), but lower compared to the TC3/IC0 subgroup (ORR 40%) [4, 13]. Therefore, it would be interesting to investigate if restoring this impairment might improve the benefit on PD-1 blockade in these patients.

For the PD-L1 staining, the SP142 antibody clone was used according to a validated protocol assessing PD-L1 expression on IC in addition to TC [3, 4]. This enabled a thorough assessment of the differences and overlap between PD-L1 expression on TC versus IC. However, in the Blueprint analysis comparing four PD-L1 IHC assays, the SP142 staining differed significantly by producing a weaker staining on TC and fewer PD-L1 positive TCs compared to the other three assays (22C3, 28-8 and SP263), which were similar in the analytical performance [14]. Based on these differences between the assays it's possible that some of the TC positive tumors may have been unjustly qualified as a TC0 tumor in our cohort in comparison with other PD-L1 assays. This may have resulted in an underestimation of the finding of a hampered IFN γ -PD-L1 axis in our TC0 subgroup and might help explain why we did not find this impairment in the TC0/IC2 or TC0/IC1 subgroup.

In conclusion, these results show the important contribution of PD-L1 expression on IC to identify inflamed tumors. Impaired IFN γ response signaling in tumor cells may explain the absence of PD-L1 expression on TC in the context of an activated immune infiltrate as represented by high PD-L1 IC positivity. These findings may help towards a better understanding of the tumor-immune system interaction and also signify the clinical relevance of PD-L1 expression on IC as a biomarker for immunotherapy in NSCLC patients.

References

1. Topalian, S.L., et al., *Safety, activity, and immune correlates of anti-PD-1 antibody in cancer*. N Engl J Med, 2012. **366**(26): p. 2443-54.
2. Garon, E.B., et al., *Pembrolizumab for the treatment of non-small-cell lung cancer*. N Engl J Med, 2015. **372**(21): p. 2018-28.
3. Fehrenbacher, L., et al., *Atezolizumab versus docetaxel for patients with previously treated non-small-cell lung cancer (POPLAR): a multicentre, open-label, phase 2 randomised controlled trial*. Lancet, 2016. **387**(10030): p. 1837-46.
4. Rittmeyer, A., et al., *Atezolizumab versus docetaxel in patients with previously treated non-small-cell lung cancer (OAK): a phase 3, open-label, multicentre randomised controlled trial*. Lancet, 2016.
5. Herbst, R.S., et al., *Predictive correlates of response to the anti-PD-L1 antibody MPDL3280A in cancer patients*. Nature, 2014. **515**(7528): p. 563-7.
6. Hegde, P.S., V. Karanikas, and S. Evers, *The Where, the When, and the How of Immune Monitoring for Cancer Immunotherapies in the Era of Checkpoint Inhibition*. Clin Cancer Res, 2016. **22**(8): p. 1865-74.
7. Goldstraw, P., et al., *The IASLC Lung Cancer Staging Project: proposals for the revision of the TNM stage groupings in the forthcoming (seventh) edition of the TNM Classification of malignant tumours*. J Thorac Oncol, 2007. **2**(8): p. 706-14.
8. Schats, K.A., et al., *Validated programmed cell death ligand 1 immunohistochemistry assays (E1L3N and SP142) reveal similar immune cell staining patterns in melanoma when using the same sensitive detection system*. Histopathology, 2017. **70**(2): p. 253-63.
9. Vennapusa, B., et al., *Development of a PD-L1 Complementary Diagnostic Immunohistochemistry Assay (SP142) for Atezolizumab*. AIMM 2019. **27**(2): p. 92-100.
10. Patel, R., et al., *Mutation scanning using MUT-MAP, a high-throughput, microfluidic chip-based, multi-analyte panel*. PloS One, 2012. **7**(12): p. e51153.
11. Schleifman, E.B., et al., *Next generation MUT-MAP, a high-sensitivity high-throughput microfluidics chip-based mutation analysis panel*. PloS One, 2014. **9**(3): p. e90761.
12. Schaake, E.E., et al., *Tumor response and toxicity of neoadjuvant erlotinib in patients with early-stage non-small-cell lung cancer*. J Clin Oncol 2012. **30**(22): p. 2731-8.
13. Kowanetz, M., et al., *Differential regulation of PD-L1 expression by immune and tumor cells in NSCLC and the response to treatment with atezolizumab (anti-PD-L1)*. Proc Natl Acad Sci U S A, 2018. **115**(43): p. E10119-e26.
14. Hirsch, F.R., et al., *PD-L1 Immunohistochemistry Assays for Lung Cancer: Results from Phase 1 of the "Blueprint PD-L1 IHC Assay Comparison Project"*. J Thorac Oncol, 2016.

SUPPLEMENTARY DATA

Table S1. List of hotspot mutations.

Gene	COSMIC ID	cDNA mutation	AA mutation	Gene	COSMIC ID	cDNA mutation	AA mutation
EGFR	6252	2155 G>A	G719S	BRAF	473	c.1798_1799GT>AA	V600K
EGFR	6253	2155 G>T	G719C	BRAF	476	c.1799T>A	V600E
EGFR	6239	2156 G>C	G719A	NRAS	565	c.35G>C	G12A
EGFR	26038	2233_2247del15	K745_E749del	NRAS	562	c.34G>T	G12C
EGFR	13550	2235_2248>AATTC	E746_A750>IP	NRAS	561	c.34G>C	G12R
EGFR	6223	2235_2249del15	E746_A750del	NRAS	563	c.34G>A	G12S
EGFR	13552	2235_2251>AATTC	E746_T751>IP	NRAS	566	c.35G>T	G12V
EGFR	13551	2235_2252>AAT	E746_T751>I	NRAS	564	c.35G>A	G12D
EGFR	12385	2235_2255>AAT	E746_S752>I	NRAS	575	c.38G>C	G13A
EGFR	12413	2236_2248>AGAC	E746_A750>RP	NRAS	570	c.37G>T	G13C
EGFR	6225	2236_2250del15	E746_A750del	NRAS	573	c.38G>A	G13D
EGFR	12728	2236_2253del18	E746_T751del	NRAS	569	c.37G>C	G13R
EGFR	12678	2237_2251del15	E746_T751>A	NRAS	574	c.38G>T	G13V
EGFR	12386	2237_2252>T	E746_T751>V	NRAS	580	c.181C>A	Q61K
EGFR	12416	2237_2253>TTGCT	E746_T751>VA	NRAS	584	c.182A>G	Q61R
EGFR	12367	2237_2254del18	E746_S752>A	NRAS	583	c.182A>T	Q61L
EGFR	12384	2237_2255>T	E746_S752>V	NRAS	582	c.182A>C	Q61P
EGFR	18427	2237_2257>TCT	E746_P753>VS	NRAS	586	c.183A>C	Q61H
EGFR	12422	2238_2248>GC	L747_A750>P	NRAS	585	c.183A>T	Q61H
EGFR	23571	2238_2252del15	L747_T751del	AKT1	33765	c.49G>A	E17K
EGFR	12419	2238_2252>GCA	L747_T751>Q	FLT3	785	c.2503G>C	D835H
EGFR	6220	2238_2255del18	E746_S752>D	FLT3	783	c.2503G>T	D835Y
EGFR	6218	2239_2247del9	L747_E749del	FLT3	784	c.2504A>T	D835V
EGFR	12382	2239_2248TTAAGAGAAG>C	L747_A750>P	FLT3	788	c.2505T>G	D835E
EGFR	12383	2239_2251>C	L747_T751>P	HRAS	480	c.34G>A	G12S
EGFR	6254	2239_2253del15	L747_T751del	HRAS	481	c.34G>T	G12C
EGFR	6255	2239_2256del18	L747_S752del	HRAS	483	c.35G>T	G12V
EGFR	12403	2239_2256>CAA	L747_S752>Q	HRAS	484	c.35G>A	G12D
EGFR	12387	2239_2258>CA	L747_P753>Q	HRAS	487	c.37G>A	G13S
EGFR	6210	2240_2251del12	L747_T751>S	HRAS	486	c.37G>C	G13R
EGFR	12369	2240_2254del15	L747_T751del	HRAS	496	c.181C>A	Q61K
EGFR	12370	2240_2257del18	L747_P753>S	HRAS	499	c.182A>G	Q61R
EGFR	13556	2253_2276del24	S752_I759del	HRAS	498	c.182A>T	Q61L
EGFR	6241	2303 G>T	S768I	HRAS	503	c.183G>C	Q61Hc
EGFR	12376	2307_2308 ins 9 (gccagcgtg)	V769_D770insASV	HRAS	502	c.183G>T	Q61Ht
EGFR	13558	2309_2310complex (ac>ccagcgtggat)	V769_D770insASV	KIT	1216	c.1669T>A	W557R
EGFR	12378	2310_2311 ins GGT	D770_N771insG	KIT	1219	c.1669T>C	W557G
EGFR	13428	2311_2312 ins 9 (gcgTggaca)	D770_N771insSVD	KIT	1290	c.1727T>C	L576P

EGFR	12377	2319_2320 ins CAC	H773_V774insH	KIT	1304	c.1924A>G	K642E
EGFR	6240	2369 C>T	T790M	KIT	12706	c.1961T>C	V654A
EGFR	6224	2573 T>G	L858R	KIT	1311	c.2446G>C	D816H
EGFR	12429	2573-2574TG>GT	L858R	KIT	1310	c.2446G>T	D816Y
EGFR	6213	2582 T>A	L861Q	KIT	1314	c.2447A>T	D816V
PIK3CA	746	c.263G>A	R88Q	MET	710	c.1124A>G	N375S
PIK3CA	754	c.1035T>A	N345K	MET	707	c.3029C>T	T1010I
PIK3CA	757	c.1258T>C	C420R	MET	699	c.3743A>G	Y1248C
PIK3CA	760	c.1624G>A	E542K	MET	700	c.3757T>G	Y1253D
PIK3CA	763	c.1633G>A	E545K	JAK2	12600	c.1849G>T	V617F
PIK3CA	12458	c.1634A>C	E545A	MYD88	85940	c.794T>C	L256P
PIK3CA	764	c.1634A>G	E545G	ERBB2	14060	c.2264T>C	L755S
PIK3CA	765	c.1635G>T	E545D	ERBB2	683	c.2263_2264TT>CC	L755P
PIK3CA	766	c.1636C>A	Q546K	ERBB2	14062	c.2329G>T	L777L
PIK3CA	6147	c.1636C>G	Q546E	KRAS	520	c.35G>T	G12V
PIK3CA	12459	c.1637A>G	Q546R	KRAS	532	c.38G>A	G13D
PIK3CA	25041	c.1637A>T	Q546L	KRAS	512	c.34_35GG>TT	G12F
PIK3CA	773	c.3129G>T	M1043I	KRAS	533	c.38G>C	G13A
PIK3CA	12591	c.3127A>G	M1043V	KRAS	527	c.37G>T	G13C
PIK3CA	776	c.3140A>T	H1047L	KRAS	529	c.37G>C	G13R
PIK3CA	775	c.3140A>G	H1047R	KRAS	528	c.37G>A	G13S
PIK3CA	774	c.3139C>T	H1047Y	KRAS	534	c.38G>T	G13V
PIK3CA	12597	c.3145G>C	G1049R	KRAS	554	c.183A>C	Q61H
KRAS	522	c.35G>C	G12A	KRAS	555	c.183A>T	Q61H
KRAS	516	c.34G>T	G12C	KRAS	549	c.181C>A	Q61K
KRAS	521	c.35G>A	G12D	KRAS	553	c.182A>T	Q61L
KRAS	517	c.34G>A	G12S	KRAS	552	c.182A>G	Q61R
KRAS	518	c.34G>C	G12R	KRAS	520	c.35G>T	G12V

Table S2. Clinicopathological features in TC3/IC<3 vs TC<3/IC3 samples.

Total (n = 125)	TC3/IC<3 36	TC<3/IC3 89	p-value
Gender			
Male	15 (41.7%)	45 (50.6%)	.43
Female	21 (58.3%)	44 (49.5%)	
Median age at surgery (years, range)	59 (39-77)	64 (36-82)	.057
Smoking			
Light smokers <10PY	1 (2.8%)	0	.32
Heavy smokers \geq 10PY	32 (88.9%)	70 (78.7%)	
Unknown	3 (8.3%)	19 (21.3%)	
Histology			
Adenocarcinoma	15 (41.6%)	52 (58.4%)	.14
Squamous cell carcinoma	20 (55.6%)	33 (37.1%)	
NSCLC NOS	1 (2.8%)	4 (4.5%)	
Tumor stage at resection			
Stage I	21 (58.3%)	40 (45.0%)	.29
Stage II	9 (25.0%)	30 (33.7%)	
Stage III	5 (13.9%)	17 (19.1%)	
Stage IV	1 (2.8%)	2 (2.3%)	
Genetic alterations			
<i>EGFRm</i>	0	2 (2.2%)	.09
<i>KRASm</i>	11 (30.1%)	19 (21.3%)	.71

Figure S1. Examples of PD-L1 co-staining of TC and IC positivity in various subgroups.

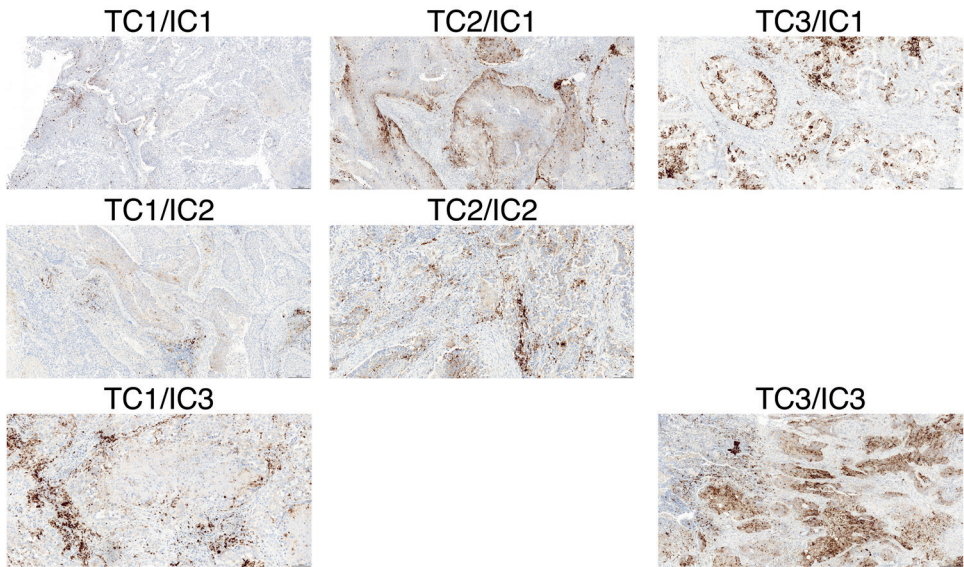


Figure S2. Percentages in Venn diagrams represent the overlap of PD-L1 expression of the TC3 with IC3, the TC2 with IC2 and the TC1 with IC1 subgroups.

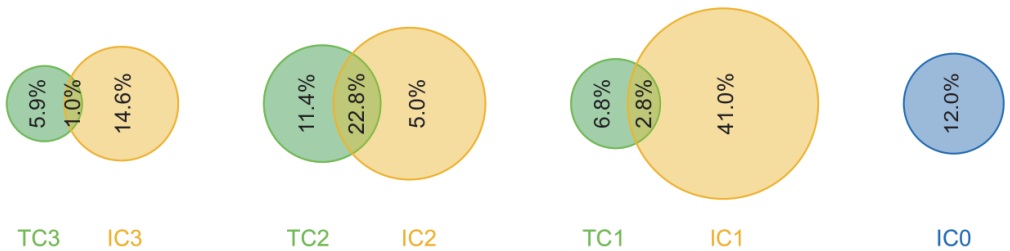
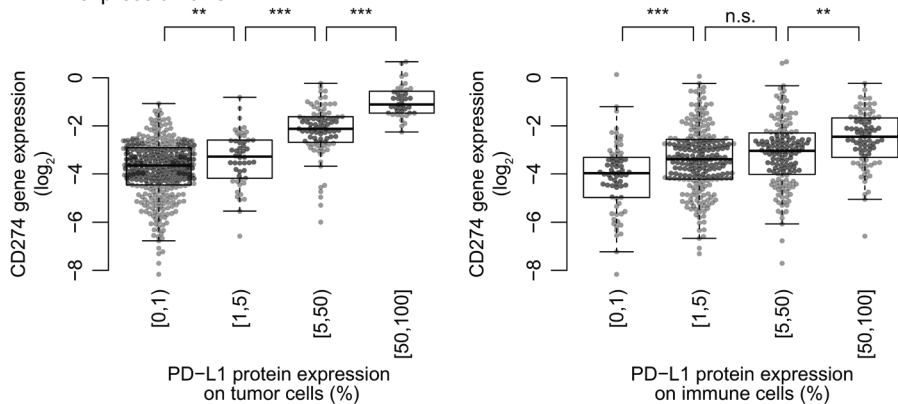
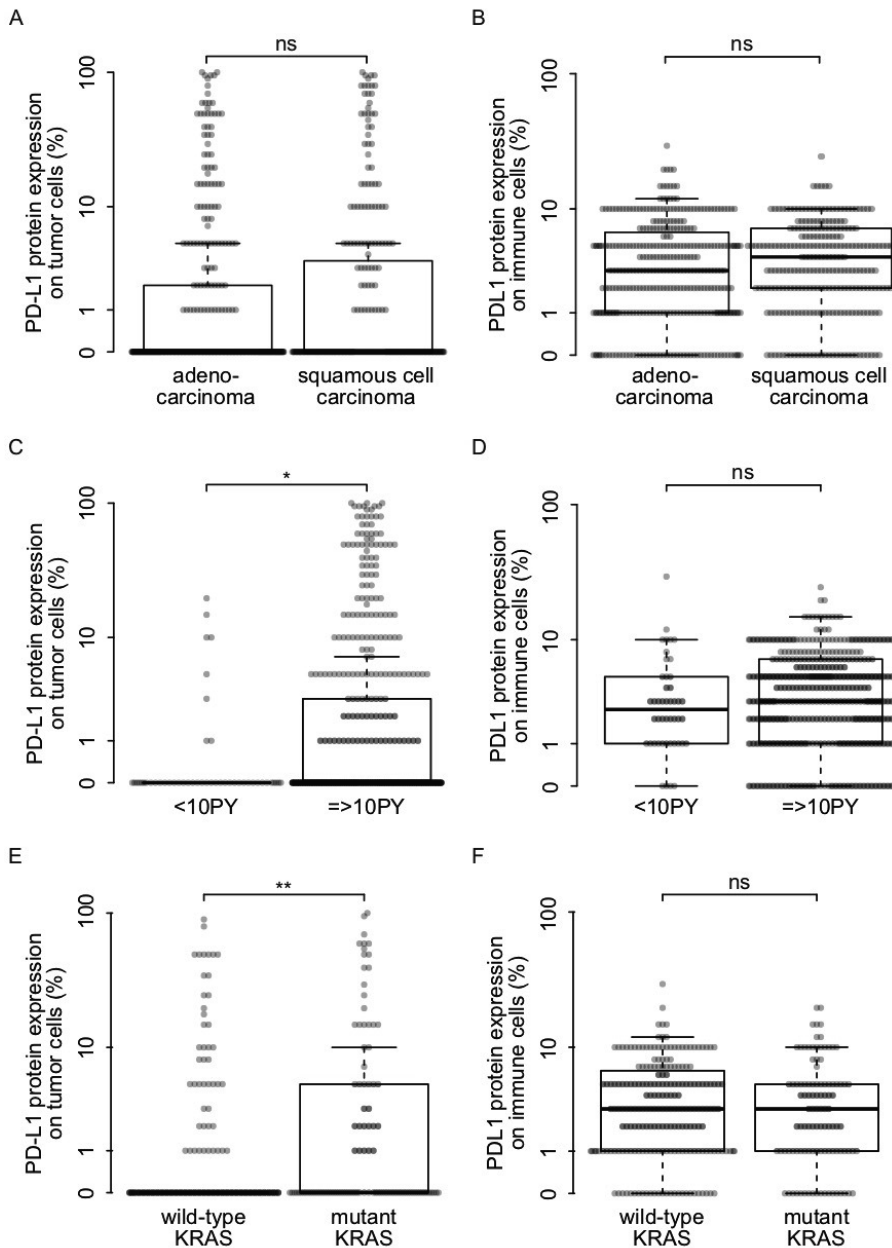


Figure S4. Associations of PD-L1 protein expression on TC and IC in non-overlapping subgroups with mRNA expression of *CD274*.



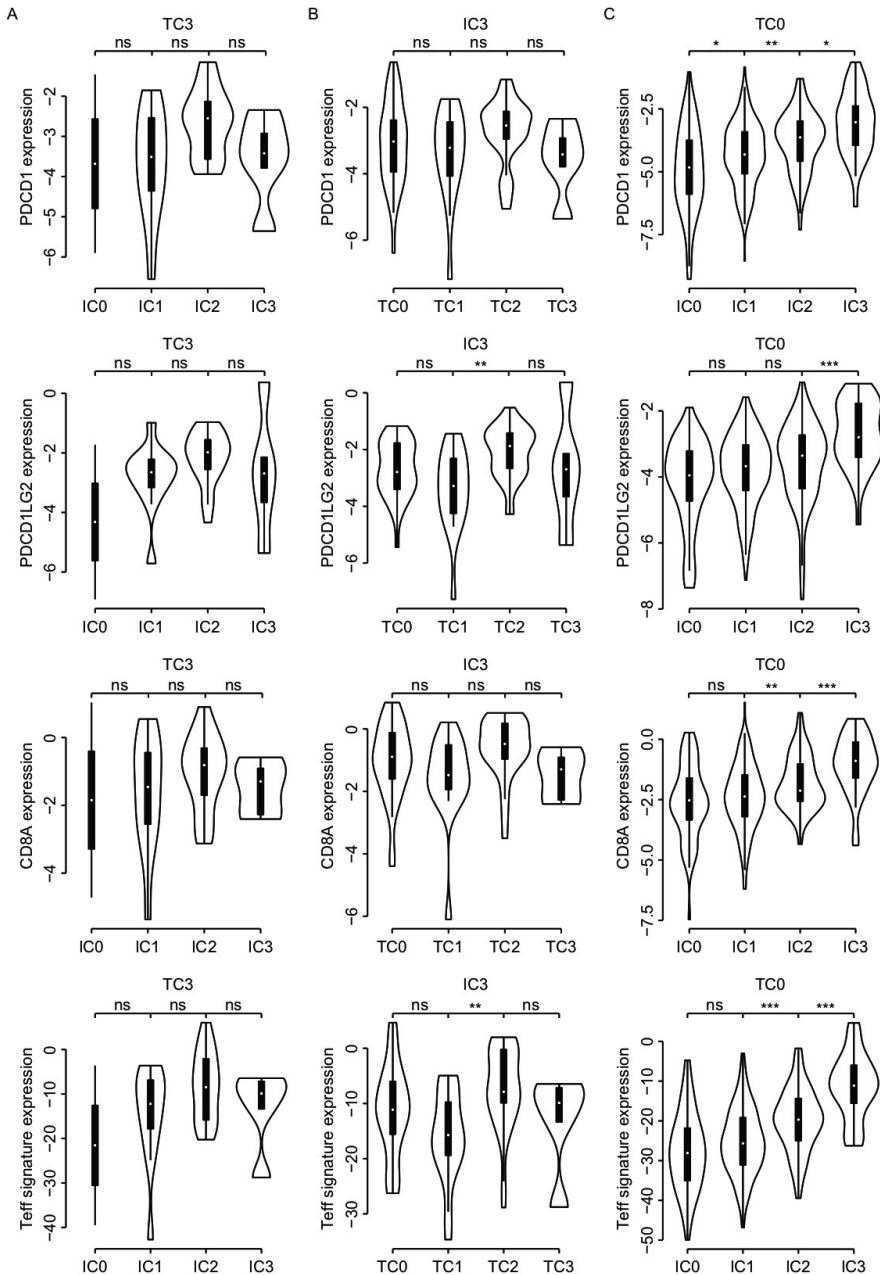
ns = non significant, ** $p < 0.01$, *** $p < 0.001$

Figure S3. PD-L1 expression on TC and IC and associations with histology, smoking and *KRAS* status.



(A, B) No significant difference was seen between SCC compared to AC regarding PD-L1 protein expression on TC or IC (n = 615). (C) PD-L1 protein expression on TC is significantly higher in heavy compared to light smokers (n = 526). (D) No significant difference was seen between heavy compared to light smokers regarding PD-L1 protein expression on IC (n = 526). (E) PD-L1 protein expression on TC is significantly higher in *KRAS**Sm* compared to *KRAS**Wt* samples in the AC cohort only (n = 317). (F) No significant difference was seen between *KRAS**Sm* compared to *KRAS**Wt* samples regarding PD-L1 expression on IC in the AC cohort only (n = 317). All boxplots were plotted on a hyperlog-transformed y-axis (see Materials and Methods). * p = 0.016, ** p < 0.001, univariate analysis. AC = adenocarcinoma, SCC = squamous cell carcinoma.

Figure S5. Associations of mRNA expression of *PDCD1*, *PDCD1LG2*, *CD8A* and the T_{eff} signature in non-overlapping PD-L1 expressing subgroups.



(A) Relative mRNA expression of *PDCD1*, *PDCD1LG2*, *CD8A* and the T_{eff} signature in TC3 tumors based on various levels of IC (n = 39). (B) Relative mRNA expression of *PDCD1*, *PDCD1LG2*, *CD8A* and the T_{eff} signature in IC3 tumors based on various levels of TC (n = 83). (C) Relative mRNA expression of the *PDCD1*, *PDCD1LG2*, *CD8A* and the T_{eff} signature in TC0 tumors based on various levels of IC (n = 351). ns = non significant, * p = 0.01 - 0.05, ** p < 0.01, *** p < 0.001

Figure S6. Expression of the T_{eff} signature vs the expression of the IFN γ response signature.

